

JINR E2-95-511
FAU-TP3-95/13
hep-ph/9512324

Photoproduction of neutral pion pairs in the Coulomb field of the nucleus

A A Bel'kov† §, M Dillig‡ and A V Lanyov†

† Particle Physics Laboratory, Joint Institute for Nuclear Research, 141980 Dubna,
Moscow Region, Russia

‡ Institut für Theoretische Physik III der Universität Erlangen-Nürnberg, D-91058
Erlangen, Germany

Abstract.

The total cross section for Coulomb photoproduction of neutral pion pairs in the reaction $\gamma A \rightarrow \pi^0 \pi^0 A$ is estimated within the effective chiral lagrangian approach. The amplitude of $\gamma \gamma^* \rightarrow \pi^0 \pi^0$ with one off-shell photon is calculated at $O(p^6)$ in the momentum expansion; in addition, nuclear absorption is taken into account. Besides its experimental feasibility, the results of the calculation demonstrate that the reaction $\gamma A \rightarrow \pi^0 \pi^0 A$ is a powerful source of information on the process $\gamma \gamma \rightarrow \pi^0 \pi^0$ close to threshold.

PACS numbers: 11.30.Rd, 13.75.Lb, 14.40.Aq, 14.80.Am

Short title:

September 27, 2018

§ E-mail: belkov@cv.jinr.dubna.su

1. Introduction

The nucleus Coulomb interaction method is an effective approach to study in high-energy experiments the low-energy electromagnetic properties of pions in the process $\gamma\gamma \rightarrow \pi\pi$. There are two possible ways to realize the Coulomb interaction method in experiment: the radiative scattering $\pi A \rightarrow \pi\gamma A$ of a pion on a nucleus and the photoproduction of pion pairs in the Coulomb field of a nucleus $\gamma A \rightarrow \pi\pi A$. The experiments under discussion are based on the fact that for sufficiently small momentum transfers the interaction of high-energy particle with nuclei is extremely peripheral and thus dominated by scattering on the virtual photons of the Coulomb field of the nucleus. The reaction $\pi A \rightarrow \pi\gamma A$ allows to investigate the $\gamma\gamma \rightarrow \pi\pi$ process in the region $m_{\pi\pi}^2 = (p_{\pi 1} + p_{\pi 2})^2 < 0$ and to measure the charged pion polarizability [1] at the point $m_{\pi\pi}^2 = 0$, while the reaction $\gamma A \rightarrow \pi\pi A$ occurs in the region $m_{\pi\pi}^2 \geq 4m_\pi^2$ close to threshold. In the case of charged pions the two reactions give complementary information about the process $\gamma\gamma \rightarrow \pi^+\pi^-$ in both the physical and the non-physical region. In the case of neutral pions the photoproduction of a neutral pion pair in the Coulomb field of a nucleus provides a new source of the information on the process $\gamma\gamma \rightarrow \pi^0\pi^0$, which was measured in the electron-positron experiment by the Crystal Ball Collaboration [2] and is under active discussion in the context of the physical programme at DAΦNE [3].

The present theoretical interest in the elementary process $\gamma\gamma \rightarrow \pi^0\pi^0$ is caused both by experimental data [2] mentioned above and recent progress in Chiral Perturbation Theory (ChPT) [4] up to and including $O(p^6)$. The process $\gamma\gamma \rightarrow \pi^0\pi^0$ is very sensitive to the higher-order contributions in ChPT since the first non-vanishing amplitude arises from meson loops at $O(p^4)$ without counterterms. However, the one-loop amplitude at $O(p^4)$ calculated in paper [5] does not describe the data even near threshold [6]. This is not surprising, as the analysis of the $\gamma\gamma \rightarrow \pi^0\pi^0$ amplitude based on dispersion relations [7] demonstrates the importance of unitarity corrections corresponding to higher orders, next to $O(p^4)$. In fact, the two-loop calculation at $O(p^6)$ carried out in paper [8] gives a considerable improvement of the description within ChPT. For completeness we mention that there is also another consideration of $\gamma\gamma \rightarrow \pi^0\pi^0$ up to one-loop order corresponding to $O(p^5)$ in the treatment of Generalized ChPT [9].

The contribution from the $O(p^6)$ counterterms was estimated in paper [8] † from the low-energy meson phenomenology with resonance exchange saturation. In papers [10, 11] the counterterms were fixed as effective meson lagrangians with higher-order derivative terms obtained from the bosonization of Nambu–Jona-Lasinio model (NJL). The sensitivity of $\gamma\gamma \rightarrow \pi^0\pi^0$ to higher-order corrections including Born

† The same paper presents a diagrammatical expansion of the amplitude $\gamma\gamma \rightarrow \pi^0\pi^0$ up to $O(p^6)$.

contributions from the effective meson lagrangian at $O(p^6)$ makes this process a valuable source of the experimental information essential for the test of bosonized chiral lagrangians at $O(p^6)$.

In this paper we investigate the possibility of studying the process $\gamma\gamma \rightarrow \pi^0\pi^0$ near threshold in the photoproduction of neutral pion pairs in the Coulomb field of a nucleus. For the first time the reaction $\gamma A \rightarrow \pi\pi A$ was considered in this context in paper [12] with a one-loop amplitude of $\gamma\gamma \rightarrow \pi^0\pi^0$ at $O(p^4)$. The total cross sections $\gamma A \rightarrow \pi\pi A$ were estimated for energies of the incident photon at 20 GeV and 40 GeV for momentum transfer cutoffs 5 MeV and 10 MeV, respectively. However, due to the large incident energy and small cutoff, the nuclear absorption and the offshellness of the virtual photon from the nuclear Coulomb field were not taken into account.

In this note, we extend and improve the previous calculation [12] in a consistent way: we presents results of a calculation of the nuclear Coulomb photoproduction of neutral pion pairs, where we include in the elementary amplitude $\gamma\gamma^* \rightarrow \pi^0\pi^0$ both off-shell corrections for the Coulomb virtual photon γ^* and contributions from ChPT up to $O(p^6)$, and where, in addition, nuclear structure and absorption are taken into account in the form factor for the nucleus.

2. Coulomb photoproduction

The photoproduction of a $\pi^0\pi^0$ pair in the Coulomb field of a nucleus is schematically described by the diagram in figure 1. The virtual photon $\gamma^*(q_2)$ for the interaction of the incident real photon with the stationary Coulomb field of the nucleus has zero energy and transfers only momentum: $q_2 = (0, \mathbf{q}_2)$. Then the amplitude of the reaction $\gamma(q_1)A \rightarrow \pi^0(p_1)\pi^0(p_2)A$ has the form

$$T_C = 2M_A \frac{eZ_A}{|\mathbf{q}_2|^2} F_A(q_{2t}, q_{2l}) e^\mu T_{\mu 0}^{(\gamma\gamma^* \rightarrow \pi^0\pi^0)}, \quad (1)$$

where M_A and Z are, respectively, the mass and charge of the nucleus. In (1), the nuclear form factor $F_A(q_{2t}, q_{2l})$, which includes nuclear absorption, depends on transverse and longitudinal components of the momentum transfer \mathbf{q}_2 measured relative to the momentum \mathbf{q}_1 of the incident photon (F_A is normalized to $F_A(0, 0) = 1$). $T_{\mu 0}^{(\gamma\gamma^* \rightarrow \pi^0\pi^0)}$ is the tensor component of the amplitude of the process $\gamma(q_1)\gamma^*(q_2) \rightarrow \pi^0(p_1)\pi^0(p_2)$.

From Lorentz and gauge invariances the general parameterization for the amplitude $T_{\mu 0}^{(\gamma\gamma^* \rightarrow \pi^0\pi^0)}$ at $O(p^6)$ has the form

$$T_{\mu\nu}^{(\gamma\gamma^* \rightarrow \pi^0\pi^0)} = A(s, t, u; q_2^2) \left(\frac{\tilde{s}}{2} g_{\mu\nu} - q_{2\mu} q_{1\nu} \right) \\ + B(s, t, u; q_2^2) \left[2\tilde{s} \Delta_\mu \Delta_\nu - \nu^2 g_{\mu\nu} - 2\nu (\Delta_\mu q_{1\nu} - q_{2\mu} \Delta_\nu) \right]$$

$$+ D(s, t, u; q_2^2) \left[\nu q_{2\mu} q_{2\nu} + \tilde{s} \Delta_\mu q_{2\nu} - q_2^2 (\nu g_{\mu\nu} + 2\Delta_\mu q_{1\nu}) \right], \quad (2)$$

where $\Delta_\mu = (p_1 - p_2)_\mu$, $s = (q_1 + q_2)^2 = (p_1 + p_2)^2$, $\tilde{s} = s - q_2^2$, $t = (p_1 - q_1)^2 = (q_2 - p_2)^2$, $u = (p_2 - q_1)^2 = (q_2 - p_1)^2$ and $\nu = t - u$.

The differential cross section for the photoproduction of a neutral pion pair in the Coulomb field of a nucleus is defined as

$$d\sigma_C^{(\gamma A \rightarrow \pi\pi A)} = \frac{\delta^{(3)}(\mathbf{p}_1 + \mathbf{p}_2 - \mathbf{q}_1 - \mathbf{q}_2) \delta(E_1 + E_2 - \varepsilon)}{4\varepsilon M_A (2\pi)^5 8E_1 E_2 M_A} \frac{1}{2} |T_C|^2 d^3\mathbf{p}_1 d^3\mathbf{p}_2 d^3\mathbf{q}_2$$

where E_i and \mathbf{p}_i ($i = 1, 2$) and ε are the energies and momenta of the pions and the energy of incident real photon, respectively. For large energies of the incident real photon and for small momentum transfers $|\mathbf{q}_2|$ to the recoil nucleus and neglecting the offshellness of the Coulomb photon and nuclear corrections, the method of equivalent photons [13] allows us to relate the differential cross section for photoproduction of pion pairs on nuclei to the total cross section for the process $\gamma\gamma \rightarrow \pi\pi$:

$$\frac{d\sigma_C^{(\gamma A \rightarrow \pi\pi A)}}{ds} = \frac{\alpha}{\pi} Z^2 \log\left(\frac{\sqrt{s}}{2m_\pi}\right) \frac{1}{s} \sigma^{(\gamma\gamma \rightarrow \pi\pi)}(s), \quad (3)$$

where $s \equiv m_{\pi\pi}^2$. In this limit equation (3) enables us to extract model-independent information on the process $\gamma\gamma \rightarrow \pi\pi$ from the experimental data on the nuclear Coulomb photoproduction of pion pairs. For a more general kinematics, the nuclear form factor and the offshellness of the Coulomb photon have to be taken into account, however.

The nuclear form factor $F_A(q_{2t}, q_{2l})$ in (1) can be estimated in the same approximation as in paper [14] since the amplitude of Coulomb photoproduction on a single proton at small q_{2t} is – upon evaluating (2) – proportional to q_{2t} :

$$\epsilon^\mu T_{\mu 0}^{(\gamma\gamma^* \rightarrow \pi^0\pi^0)} \approx (\epsilon \cdot q_{2t}) \left[A - 2\left(\tilde{s}(E_1 - E_2) - \nu\varepsilon + 2\nu(E_1 - E_2)\right) B - 2\varepsilon D \right].$$

In the approach of paper [14] the nucleus is treated as a completely absorbing sphere, with the form factor

$$F_A(q_t, q_l) = q_l R J_0(q_t R) K_1(q_l R) + \frac{(q_l R)^2}{q_l R} J_1(q_t R) K_0(q_l R) + \Delta F_A(q_t, q_l), \quad (4)$$

where R is the radius of the nucleus, and J_n and K_n ($n = 0, 1$) are Bessel functions. In our estimates R is chosen to be $R = 1.12A^{1/3}$ fm, where A is atomic weight of a nucleus. The first two terms in (4) arise from the integration over the three-dimensional space outside a cylinder of radius R of the nucleus. They reflect the assumption, that the nucleus is completely ‘black’ for the outgoing pions for impact parameters $b \leq R$, resulting in a cut $\theta(b - R)$, in the profile function. This drastic assumption is mediated by the correction term $\Delta F_A(q_t, q_l)$, which arises from the

integration over the three-dimensional cylinder behind the nucleus and corresponds to the interaction of photons with the nuclear Coulomb field after passing through the nucleus.

In general, the integrations above can be done only numerically. However, when both $(q_l R)$ and $(q_t R)$ are small compared to unity, the correction $\Delta F_A(q_t, q_l)$ can conveniently be expanded to obtain

$$\begin{aligned} \Delta F_A(q_t, q_l) = \frac{1}{4} \left\{ 1 - q_l R J_0(q_t R) K_1(q_l R) - \frac{(q_l R)^2}{q_t R} J_1(q_t R) K_0(q_l R) \right. \\ + [(q_l R)^2 + (q_t R)^2] \left(-\frac{1}{6} + \frac{i}{8} q_l R + \frac{1}{120} (q_t R)^2 \right. \\ \left. \left. + \frac{4 - i15\pi}{480} (q_l R)^2 + i \frac{5}{144} (q_l R)^3 - \frac{i}{96} q_l R (q_t R)^2 \right) + \dots \right\}. \end{aligned}$$

3. Chiral lagrangians

The calculation of the amplitude of $\gamma\gamma^* \rightarrow \pi^0\pi^0$ at $O(p^6)$ of the momentum expansion of ChPT involves tree-level, one-loop and two-loop diagrams of a chiral effective lagrangian. The effective meson lagrangian at $O(p^2)$ can be written in the nonlinear parameterization of chiral $SU(2) \times SU(2)$ symmetry as

$$\mathcal{L}_{\text{eff}}^{(2)} = \frac{F_0^2}{4} \text{tr} (D_\mu U \bar{D}^\mu U^\dagger) + \frac{F_0^2}{4} \text{tr} (\chi U^\dagger + U \chi^\dagger), \quad (5)$$

where

$$U(x) = \exp \left(\frac{i}{F_0} \varphi(x) \right), \quad \varphi = \begin{pmatrix} \pi^0 & \sqrt{2}\pi^+ \\ \sqrt{2}\pi^- & -\pi^0 \end{pmatrix} \quad (6)$$

represents the pseudoscalar degrees of freedom, F_0 is the bare π decay constant, and $\chi = \text{diag}(\chi_u^2, \chi_d^2)$ is the mass matrix. The covariant derivatives D_μ and \bar{D}_μ contain the vector and axial-vector degrees of freedom, and are defined as

$$D_\mu U = \partial_\mu U + (A_\mu^L U - U A_\mu^R), \quad \bar{D}_\mu U^\dagger = \partial_\mu U^\dagger + (A_\mu^R U^\dagger - U^\dagger A_\mu^L),$$

where $A_\mu^{R/L} = V_\mu \pm A_\mu$ are the right/left combinations of vector and axial-vector fields. The interaction with the electromagnetic field \mathcal{A}_μ can be included by replacing $V_\mu \rightarrow V_\mu + ie\mathcal{A}_\mu Q$, where Q is the matrix of quark electric charges.

The effective meson Lagrangian of $O(p^4)$ is presented in the general form with structure coefficients L_i and H_i introduced by Gasser and Leutwyler in paper [4],

$$\begin{aligned} \mathcal{L}_{\text{eff}}^{(4)} = & \left(L_1 - \frac{1}{2} L_2 \right) (\text{tr} L_\mu L^\mu)^2 + L_2 \text{tr} \left(\frac{1}{2} [L_\mu, L_\nu]^2 + 3(L_\mu L^\mu)^2 \right) \\ & + L_3 \text{tr} ((L_\mu L^\mu)^2) - L_4 \text{tr} (L_\mu L^\mu) \text{tr} (\chi U^\dagger + U \chi^\dagger) \\ & - L_5 \text{tr} [L_\mu L^\mu (\chi U^\dagger + U \chi^\dagger)] + L_6 \left(\text{tr} (\chi U^\dagger + U \chi^\dagger) \right)^2 \end{aligned}$$

$$\begin{aligned}
& + L_7 \left(\text{tr}(\chi U^\dagger - U \chi^\dagger) \right)^2 + L_8 \text{tr}(\chi U^\dagger \chi U^\dagger + U \chi^\dagger U \chi^\dagger) \\
& - L_9 \text{tr} \left(F_{\mu\nu}^R R^\mu R^\nu + F_{\mu\nu}^L L^\mu L^\nu \right) - L_{10} \text{tr} \left(U F_{\mu\nu}^R U^\dagger F^{L\mu\nu} \right) \\
& - H_1 \text{tr} \left((F_{\mu\nu}^R)^2 + (F_{\mu\nu}^L)^2 \right) + H_2 \text{tr}(\chi \chi^\dagger). \tag{7}
\end{aligned}$$

In equation (7), $L_\mu = D_\mu U \cdot U^\dagger$, $R_\mu = U^\dagger D_\mu U$, and $F_{\mu\nu}^{R/L} = F_{\mu\nu}^V \pm F_{\mu\nu}^A$ are the right/left combinations of the field strength tensors

$$F_{\mu\nu}^V = \partial_\mu V_\nu - \partial_\nu V_\mu + [V_\mu, V_\nu] + [A_\mu, A_\nu], \quad F_{\mu\nu}^A = \partial_\mu A_\nu - \partial_\nu A_\mu + [V_\mu, A_\nu] + [A_\mu, V_\nu].$$

It is convenient to present the part of the effective lagrangian at $O(p^6)$ for $\gamma\gamma \rightarrow \pi^0\pi^0$ with structure coefficients d_i ,

$$\begin{aligned}
\mathcal{L}_6 = \frac{8}{F_0^2} & \left[d_1 \mathcal{F}_{\mu\alpha} \mathcal{F}^{\mu\beta} \text{tr} \left(\partial^\alpha U_0 \partial_\beta U_0^\dagger Q^2 \right) + d_2 \mathcal{F}_{\mu\nu} \mathcal{F}^{\mu\nu} \text{tr} \left(\partial_\alpha U_0 \partial^\alpha U_0^\dagger Q^2 \right) \right. \\
& + d_3 \mathcal{F}_{\mu\nu} \mathcal{F}^{\mu\nu} \text{tr} \left(\chi (U_0 + U_0^\dagger) Q^2 \right) + d_4 \mathcal{F}_{\mu\nu} \mathcal{F}^{\mu\nu} \text{tr} (Q^2) \text{tr} \left(\chi (U_0 + U_0^\dagger) \right) \\
& + d_5 \mathcal{F}_{\mu\alpha} \mathcal{F}^{\mu\beta} \text{tr} \left(Q^2 \right) \text{tr} \left(\partial^\alpha U_0 \partial_\beta U_0^\dagger \right) + d_6 \mathcal{F}_{\mu\nu} \mathcal{F}^{\mu\nu} \text{tr} \left(Q^2 \right) \text{tr} \left(\partial_\alpha U_0 \partial^\alpha U_0^\dagger \right) \\
& + d_7 \mathcal{F}_{\mu\alpha} \mathcal{F}^{\mu\beta} \text{tr} \left(\partial^\alpha U_0 U_0^\dagger Q \right) \text{tr} \left(\partial_\beta U_0 U_0^\dagger Q \right) \\
& \left. + d_8 \mathcal{F}_{\mu\nu} \mathcal{F}^{\mu\nu} \text{tr} \left(\partial_\alpha U_0 U_0^\dagger Q \right) \text{tr} \left(\partial^\alpha U_0 U_0^\dagger Q \right) \right], \tag{8}
\end{aligned}$$

where $\mathcal{F}_{\mu\nu} = \partial_\mu A_\nu - \partial_\nu A_\mu$ is the standard electromagnetic field strength tensor, and $U_0 = \exp(i\varphi_0/F_0)$, $\varphi_0 = \text{diag}(\pi^0, -\pi^0)$. The lagrangian of equation (8) can be obtained from the most general representation of the full lagrangian of paper [17].

The structure coefficients of the $O(p^4)$ and $O(p^6)$ chiral lagrangians of equations (7) and (8) can be fixed either from low-energy meson phenomenology, as in papers [4, 8], or from the bosonization of NJL-type effective quark models (see papers [15, 16, 10, 11] and references therein).

4. Amplitudes of $\gamma\gamma^* \rightarrow \pi^0\pi^0$

In general, the prediction for the Born amplitude of $\gamma\gamma^* \rightarrow \pi^0\pi^0$ at $O(p^6)$ involves eight structure coefficients d_i of the lagrangian (8). In the NJL model only the structure constants d_1, d_2, d_3 get nonzero values and contribute to the amplitude:

$$\begin{aligned}
A^{\text{B}(p^6)} &= \frac{64e^2}{9F_0^4} \left[\frac{5}{16} d_1 (s + q_2^2) + \frac{5}{2} d_2 (s - 2m_\pi^2) + d_3 (4\chi_u^2 + \chi_d^2) \right], \\
B^{\text{B}(p^6)} &= -\frac{10e^2}{9F_0^4} d_1.
\end{aligned}$$

The one-loop amplitude of $\gamma\gamma^* \rightarrow \pi^0\pi^0$ at $O(p^4)$, which has no UV divergences, is given as

$$A_\pi^{\text{1l}(p^4)} = -\frac{2e^2}{3F_0^2} \frac{1}{16\pi^2} (6s - 8m_\pi^2 + \chi_u^2 + \chi_d^2) \left[-\frac{2q_2^2}{s^2} (J_\pi^1(s) - J_\pi^1(q_2^2)) + H_\pi(s, q_2^2) \right],$$

$$B_\pi^{11(p^4)} = D_\pi^{11(p^4)} = 0,$$

with

$$H_\pi(s, q_2^2) = \frac{1}{\tilde{s}} \left[1 + \frac{2m_\pi^2}{\tilde{s}} \left(J_\pi^{-1}(s) - J_\pi^{-1}(q_2^2) \right) \right],$$

and

$$J_\pi^n(a) = \int_0^1 d^4x x^n \log \left[\frac{m_\pi^2 - a(1-x)x - i\epsilon}{m_\pi^2} \right].$$

In our approach UV divergences, resulting from meson loops at $O(p^6)$, are separated using the superpropagator regularization method [18], which is particularly well-suited for the treatment of loops in nonlinear chiral theories. The result is equivalent to the dimensional regularization technique used in paper [8], the difference being that the scale parameter μ is no longer arbitrary but fixed by the inherent scale $\tilde{\mu}$ of the chiral theory, namely, $\tilde{\mu} = 4\pi F_0$. For comparison of these two methods, the constants from the UV divergences in the dimensional regularization have to be replaced by a finite term using the substitution

$$(C-1/\varepsilon) \quad \longrightarrow \quad C_{\text{SP}} = 2C + 1 + \frac{1}{2} \left[\frac{d}{dz} \left(\log \Gamma^{-2}(2z+2) \right) \right]_{z=0} + \beta\pi = -1 + 4C + \beta\pi,$$

where $C = 0.577$ is Euler's constant, $\varepsilon = (4-D)/2$, and β is an arbitrary constant resulting from the representation of the superpropagator as an integral of the Sommerfeld-Watson type. The splitting of the decay constants F_π and F_K is used at $O(p^4)$ to fix $C_{\text{SP}} \approx 3.0$ for $F_0 = 90$ MeV.

The one-loop diagrams at $O(p^6)$ involve the structure coefficients L_i of the lagrangian (7) and give the following contributions

$$\begin{aligned} A_\pi^{11(p^6)} = & -\frac{e^2}{3F_0^4} \frac{1}{16\pi^2} \left\{ \left[2L_9 q_2^2 (6s - 8m_\pi^2 + \chi_u^2 + \chi_d^2) \right. \right. \\ & + 12L_2 (3s^2 - 8m_\pi^2 (s - m_\pi^2)) + 24(2L_1 - L_2 + L_3) (s - 2m_\pi^2)^2 \\ & + 16L_4 (3(s - 2m_\pi^2)(\chi_u^2 + \chi_d^2) - (3s - 4m_\pi^2) \text{tr}\chi) \\ & \left. - 16L_5 m_\pi^2 (\chi_u^2 + \chi_d^2) \right] 2 \left[-\frac{2q_2^2}{\tilde{s}^2} (J_\pi^1(s) - J_\pi^1(q_2^2)) + H_\pi(s, q_2^2) \right] \\ & + 4(L_9 + L_{10}) (6s - 8m_\pi^2 + \chi_u^2 + \chi_d^2) G_\pi(s) \\ & + 12L_2 \left[\frac{2}{3} J_\pi^1(s) \left(s - 2m_\pi^2 - \frac{1}{4\tilde{s}} (3q_2^4 - 48q_2^2 m_\pi^2 + 32m_\pi^4) \right. \right. \\ & \quad \left. \left. - \frac{1}{2\tilde{s}^2} (80q_2^2 m_\pi^4 - 21q_2^4 m_\pi^2 + 2q_2^6 + 6\nu^2 (q_2^2 + 12m_\pi^2)) \right. \right. \\ & \quad \left. \left. - \frac{6}{\tilde{s}^3} \nu^2 q_2^2 (q_2^2 + 19m_\pi^2) - \frac{3}{\tilde{s}^4} \nu^2 q_2^4 (q_2^2 + 26m_\pi^2) \right) \right. \\ & \left. + \frac{2}{3} J_\pi^1(q_2^2) \left(4m_\pi^4 - q_2^4 + \frac{q_2^2}{\tilde{s}} (q_2^2 - 10m_\pi^2) \right) \right\} \end{aligned}$$

$$\begin{aligned}
& + \frac{1}{\tilde{s}^2} \left(40q_2^2 m_\pi^4 - 14q_2^4 m_\pi^2 + q_2^6 + 3\nu^2 (q_2^2 + 4m_\pi^2) \right) \\
& + \frac{6}{\tilde{s}^3} \nu^2 q_2^2 (q_2^2 + 14m_\pi^2) + \frac{3}{\tilde{s}^4} \nu^2 q_2^4 (q_2^2 + 26m_\pi^2) \\
& - 2H_\pi(s, q_2^2) \left(\tilde{s}m_\pi^2 - 4m_\pi^4 + q_2^2 m_\pi^2 - \nu^2 - \frac{2}{\tilde{s}} \nu^2 (m_\pi^2 + 2q_2^2) \right. \\
& \quad \left. - \frac{3}{\tilde{s}^2} \nu^2 q_2^2 (m_\pi^2 + q_2^2) \right) \\
& - \frac{1}{18} (s - 4m_\pi^2) + \frac{1}{3\tilde{s}} (q_2^4 - 14q_2^2 m_\pi^2 - 5\nu^2) - \frac{13}{2\tilde{s}^2} \nu^2 q_2^2 \\
& \left. - \frac{5}{\tilde{s}^3} \nu^2 q_2^4 + \frac{1}{3} \tilde{C}_\pi (\tilde{s} - 4m_\pi^2) \right] \Big\}, \\
B_\pi^{11(p^6)} &= -\frac{4e^2}{F_0^4} \frac{1}{16\pi^2} L_2 \left\{ \frac{1}{3} J_\pi^1(s) \left[1 - \frac{2}{\tilde{s}} (5m_\pi^2 - q_2^2) - \frac{q_2^2}{\tilde{s}^2} (10m_\pi^2 - q_2^2) \right] \right. \\
& + \frac{1}{3\tilde{s}} J_\pi^1(q_2^2) \left[2(4m_\pi^2 - q_2^2) + \frac{q_2^2}{\tilde{s}} (10m_\pi^2 - q_2^2) \right] \\
& \left. + m_\pi^2 H_\pi(s, q_2^2) - \frac{q_2^2}{6\tilde{s}} - \frac{7}{36} + \frac{1}{6} \tilde{C}_\pi \right\}, \\
D_\pi^{11(p^6)} &= \frac{8e^2}{3F_0^4} \frac{1}{16\pi^2} L_2 \frac{\nu}{\tilde{s}^3} \left\{ q_2^2 J_\pi^1(s) \left[\tilde{s}^2 + 2\tilde{s}(13m_\pi^2 + q_2^2) + (26m_\pi^2 + q_2^2) \right] \right. \\
& + J_\pi^1(q_2^2) \left[\tilde{s}^2 (4m_\pi^2 - q_2^2) - 2\tilde{s}q_2^2 (8m_\pi^2 + q_2^2) - q_2^4 (26m_\pi^2 + q_2^2) \right] \\
& \left. - 3q_2^2 H_\pi(s, q_2^2) \tilde{s}^2 (s + m_\pi^2) + \frac{1}{4} q_2^2 \tilde{s} (9s + q_2^2) \right\},
\end{aligned}$$

where $G_\pi(s) = \tilde{C}_\pi + 2J_\pi^1(s)$ and $\tilde{C}_\pi = C_{\text{SP}} + \log \frac{m_\pi^2}{16\pi^2 F_0^2}$.

Only two-loop diagrams which are factorizable can be calculated analytically.

Their contribution can be presented in the form

$$\begin{aligned}
A_\pi^{21(p^6)} &= -\frac{2e^2}{3F_0^4} \frac{1}{(16\pi^2)^2} \left\{ J_\pi^1(q_2^2) \left(\frac{q_2^2}{\tilde{s}^2} J_\pi^1(q_2^2) + \frac{1}{2} H_\pi(s, q_2^2) \right) \frac{1}{\tilde{s}^3} \left[-\frac{32}{3} m_\pi^4 \tilde{s}^3 \right. \right. \\
& + 2s^4 (4m_\pi^2 - q_2^2) - \frac{2}{3} s^3 q_2^2 (32m_\pi^2 - 9q_2^2) + 2s^2 q_2^4 (8m_\pi^2 - 3q_2^2) \\
& \left. - 2s q_2^4 (32m_\pi^4 - q_2^4) - \frac{8}{3} m_\pi^2 q_2^8 + \frac{1}{3} \tilde{s}^3 (4m_\pi^2 - q_2^2) (\chi_u^2 + \chi_d^2) \right] \\
& - \frac{1}{3\tilde{s}^5} J_\pi^1(q_2^2) \left[6s^5 (4m_\pi^2 - q_2^2) - s^4 (20m_\pi^4 + 15m_\pi^2 q_2^2 - 29q_2^4) \right. \\
& - 16m_\pi^2 \tilde{s}^4 - \frac{2}{3} s^3 q_2^2 (16m_\pi^4 + 166m_\pi^2 q_2^2 + 9q_2^4) \\
& + 2s^2 q_2^4 (60m_\pi^4 + 91m_\pi^2 q_2^2 + 15q_2^4) \\
& - 2s q_2^6 (176m_\pi^4 + 46m_\pi^2 q_2^2 + q_2^4) + \frac{1}{3} m_\pi^2 q_2^8 (276m_\pi^2 + 35q_2^2) \\
& \left. + \frac{1}{6} \left(3(\tilde{s}^4 + s^4) (4m_\pi^2 - q_2^2) - 3s^3 q_2^2 (36m_\pi^2 - 7q_2^2) \right) \right]
\end{aligned}$$

$$\begin{aligned}
& - 24s^2q_2^4(6m_\pi^2 - q_2^2) + 6sq_2^6(20m_\pi^2 - 3q_2^2) \\
& + q_2^8(36m_\pi^2 - 5q_2^2) \left(\chi_u^2 + \chi_d^2 \right) \Big] \\
& + J_\pi^1(s) \left(\frac{q_2^2}{\tilde{s}^2} J_\pi^1(s) - \frac{1}{2} H_\pi(s, q_2^2) \right) \frac{1}{\tilde{s}^3} \left[\frac{64}{3} m_\pi^4 \tilde{s}^3 + 12s^5 \right. \\
& - 4s^4(8m_\pi^2 + 9q_2^2) + \frac{4}{3} s^3 q_2^2 (32m_\pi^2 + 9q_2^2) - 12s^2 q_2^4 (8m_\pi^2 + q_2^2) \\
& + 32sm_\pi^4 q_2^6 + \frac{16}{3} \tilde{s}^3 (3s - 4m_\pi^2) (\chi_u^2 + \chi_d^2) + \frac{7}{3} \tilde{s}^3 (\chi_u^2 + \chi_d^2)^2 \Big] \\
& + \frac{1}{3\tilde{s}^5} J_\pi^1(s) \left[6s^5 m_\pi^2 - 2s^4 (20m_\pi^4 + 88m_\pi^2 q_2^2 + 19q_2^4) + 32m_\pi^4 \tilde{s}^4 \right. \\
& + 2s^3 q_2^2 \left(136m_\pi^4 - \frac{502}{3} m_\pi^2 q_2^2 - 5q_2^4 \right) \\
& - 6s^2 q_2^4 \left(96m_\pi^4 + \frac{124}{3} m_\pi^2 q_2^2 + q_2^4 \right) \\
& + 2sq_2^6 (248m_\pi^4 + 43m_\pi^2 q_2^2 + q_2^4) - \frac{8}{3} m_\pi^2 q_2^8 (57m_\pi^2 + q_2^2) \\
& + \frac{1}{3} \left(-72s^5 + 36s^4 (3m_\pi^2 + 8q_2^2) + 24\tilde{s}^4 (3s - 4m_\pi^2) \right. \\
& - s^3 q_2^2 (420m_\pi^2 + 433q_2^2) + 3s^2 q_2^4 (204m_\pi^2 + 97q_2^2) \\
& \left. - 3sq_2^6 (132m_\pi^2 + 25q_2^2) + q_2^8 (96m_\pi^2 + q_2^2) \right) \left(\chi_u^2 + \chi_d^2 \right) \Big] \\
& + \frac{q_2^2}{\tilde{s}^5} J_\pi^1(q_2^2) J_\pi^1(s) \left[-12s^5 + 2s^4 (12m_\pi^2 + 19q_2^2) - \frac{32}{3} m_\pi^4 \tilde{s}^3 \right. \\
& - \frac{14}{3} s^3 q_2^2 (16m_\pi^2 + 3q_2^2) + 2s^2 q_2^4 (40m_\pi^2 + 9q_2^2) \\
& - 2sq_2^6 (16m_\pi^2 + q_2^2) + \frac{8}{3} m_\pi^2 q_2^8 + \frac{1}{3} \left(20m_\pi^2 \tilde{s}^3 - 48s^4 + 145s^3 q_2^2 \right. \\
& \left. - 147s^2 q_2^4 + 51sq_2^6 - q_2^8 \right) (\chi_u^2 + \chi_d^2) - \frac{7}{3} \tilde{s}^3 (\chi_u^2 + \chi_d^2)^2 \Big] \\
& - \frac{1}{2\tilde{s}^3} H_\pi(s, q_2^2) \left[-\frac{2}{3} s^4 (36m_\pi^2 + q_2^2) + \frac{2}{9} s^3 q_2^2 (328m_\pi^2 + 9q_2^2) \right. \\
& + \frac{112}{3} m_\pi^4 \tilde{s}^3 - 2s^2 q_2^4 (38m_\pi^2 + q_2^2) + \frac{2}{3} sq_2^6 (40m_\pi^2 + q_2^2) \\
& \left. - \frac{8}{9} m_\pi^2 q_2^8 + \frac{1}{9} \tilde{s}^3 (12m_\pi^2 - q_2^2) (\chi_u^2 + \chi_d^2) \right] \\
& - \frac{1}{9\tilde{s}^5} \left(s^4 q_2^2 (109m_\pi^2 + 3q_2^2) - 48m_\pi^4 \tilde{s}^4 + 2m_\pi^2 s^3 q_2^4 - 4m_\pi^2 sq_2^8 - 3m_\pi^2 q_2^{10} \right) \\
& + \tilde{C}_\pi \left(\frac{q_2^2}{\tilde{s}^2} (J_\pi^1(s) - J_\pi^1(q_2^2)) - \frac{1}{2} H_\pi(s, q_2^2) \right) \frac{1}{\tilde{s}^3} \left[6s^5 + s^4 (8m_\pi^2 - 17q_2^2) \right. \\
& \left. - \frac{1}{3} s^3 q_2^2 (76m_\pi^2 - 45q_2^2) - \frac{80}{3} m_\pi^4 \tilde{s}^3 + s^2 q_2^4 (28m_\pi^2 - q_2^2) \right]
\end{aligned}$$

$$\begin{aligned}
& -sq_2^6(12m_\pi^2 + q_2^2) + \frac{4}{3}m_\pi^2q_2^8 - \frac{1}{6}(72m_\pi^2\tilde{s}^3 - 48s^4 + 143s^3q_2^2 \\
& - 141s^2q_2^4 + 45sq_2^6 + q_2^8)(\chi_u^2 + \chi_d^2) + \frac{7}{6}s^3(\chi_u^2 + \chi_d^2)^2 \\
& + \frac{1}{\tilde{s}^5}\tilde{C}_\pi \left[s^5m_\pi^4 - \frac{23}{6}s^4m_\pi^2q_2^2 + 4m_\pi^4\tilde{s}^4 + \frac{1}{3}s^3q_2^4(3m_\pi^2 + 16q_2^2) \right. \\
& - s^2q_2^6(20m_\pi^2 + q_2^2) + \frac{1}{3}sq_2^8m_\pi^2 + \frac{1}{6}m_\pi^2q_2^{10} \\
& \left. + \frac{2}{3}m_\pi^2\tilde{s}^4(\chi_u^2 + \chi_d^2) \right] \Big\},
\end{aligned}$$

$$B_\pi^{2l(p^6)} = D_\pi^{2l(p^6)} = 0.$$

It should be stressed that additional two-loop diagrams, such as box diagrams and acnode graphs, which cannot be evaluated analytically, can be neglected: the numerical estimates in paper [8] indicate the smallness of their contributions in the photoproduction process under consideration.

5. Numerical estimates and conclusion

Monte Carlo techniques were used to compute the total cross sections for the photoproduction of $\pi^0\pi^0$ -pairs in the Coulomb field of the carbon ($Z = 6$) and silicon nuclei ($Z = 14$). It is important to note that for a momentum transfer cutoff $q_{\max} \equiv |\mathbf{q}_2|_{\max} \ll \varepsilon$, the effective mass of $\pi\pi$ system varies in the range $4m_\pi^2 \leq m_{\pi\pi}^2 \leq 2\varepsilon q_{\max}$.

The dependence of the total cross section of the reaction $\gamma A \rightarrow \pi^0\pi^0 A$ on the momentum transfer cutoff q_{\max} for different energies ε of the incident real photon is shown in figures 2 and 3. (In the calculation, the additional cutoff $m_{\pi\pi} \leq 700$ MeV was used, corresponding to the range of validity of the chiral theory.) In figure 2 we demonstrate explicitly the influence of the nuclear form factor: our numerical estimates indicate that the nuclear effects are mainly saturated by the contribution of the two first terms of equation (4), while the correction ΔF_A does not exceed 10%. For our numerical estimates we used for the parameters L_i and d_i the values from (14) and Table 1 of paper [11] obtained from the NJL model. These values include the resonance-exchange contributions effectively taken into account by integrating out the vector, axial-vector and scalar degrees of freedom. Moreover, for numerical comparison with the phenomenological approach to $\gamma\gamma \rightarrow \pi^0\pi^0$, we used the structure constants L_i and d_i corresponding to Tables 1 and 2 of paper [8]. The results of our calculations with the parameters of paper [8] are also shown in figure 2.

The main background for the Coulomb photoproduction of $\pi^0\pi^0$ pairs is the double pion photoproduction reaction on the nucleon $\gamma N \rightarrow \pi^0\pi^0 N$ via the baryon

resonance exchange mechanism [19, 20]. In the photon energy region near $\varepsilon = 1$ GeV the total cross sections of the reactions $\gamma p \rightarrow \pi^0\pi^0 p$ and $\gamma n \rightarrow \pi^0\pi^0 n$ are dominated by diagrams in figure 4 with $\Delta(1232)$ -isobar and resonance $N^*(1520)$ [21]. Kroll-Ruderman diagram dominating in other isospin channels and meson exchange diagrams do not contribute to the photoproduction of $\pi^0\pi^0$ pairs. The contributions of diagrams j, l, and n of figure 4 to the reaction $\gamma A \rightarrow \pi^0\pi^0 A$ can be canceled by choosing an isoscalar target because of opposite signs of the corresponding amplitudes on the proton and neutron. The amplitude of diagram p in figure 4 is proportional to the difference of the coupling constants $(\tilde{g}_\gamma^N - \tilde{g}_\sigma^N)$ (see paper [21] for more details). The corresponding contribution to the process $\gamma A \rightarrow \pi^0\pi^0 A$ on the isoscalar target proves to be also suppressed due to the fact that

$$(\tilde{g}_\gamma^N - \tilde{g}_\sigma^N) = \begin{cases} 0.157 & , \text{ for proton ,} \\ -0.136 & , \text{ for neutron .} \end{cases}$$

The effect of such self-cancellation of diagrams j, l, n and p from figure 4 is demonstrated in figure 5 where we present the results of our calculation of the total cross section of the double pion photoproduction reaction on the proton, neutron and on the system (proton + neutron). Numerically our calculations are in a good agreement with the results of paper [21] and in a reasonable agreement with the recent experimental data [22].

In figure 6 we also show the photon energy dependence of the total cross sections for the coherent double pion photoproduction on the carbon and silicon nuclei (isoscalar targets) calculated with the Born nuclear electromagnetic form factor with symmetrized Fermi-density [23]:

$$F_B^{SF}(q) = -\frac{4\pi^2 b R \rho^{(0)}}{q \sinh \pi b q} \left(\cos qR - \frac{\pi b}{R} \sin qR \cot \pi b q \right),$$

where $q = |\mathbf{q}_1 - \mathbf{p}_1 - \mathbf{p}_2|$. The normalization constant is defined as

$$\rho^{(0)} = \frac{3}{4\pi} \frac{1}{R(R^2 + \pi^2 b^2)},$$

and the following values of radius of the nucleus R and impact parameter b were used: $R = 2.214$ fm, $b = 0.488$ fm — for carbon, and $R = 3.085$ fm, $b = 0.563$ fm — for silicon. Our results for $\sigma_{tot}(C^{12})$ agree with recent estimates [24].

To estimate the contribution of the reaction $\gamma N \rightarrow \pi^0\pi^0 N$ to this part of the phase space which corresponds to the cutoffs introduced above for the Coulomb photoproduction of $\pi^0\pi^0$ pairs, the additional cutoffs must be also taken into account when Monte Carlo simulating the background: $m_{\pi\pi} \leq 700$ MeV and $\sqrt{-t_N} \leq q_{max}$, where $t_N = (p_1 - p_2)^2$, p_1 and p_2 are the momenta of nucleon in the initial and final states, respectively. The photon energy dependence of the cross sections for

the carbon and silicon targets calculated with the cutoffs are shown in figure 6. Our estimates of the $\gamma N \rightarrow \pi^0 \pi^0 N$ background have shown that in the case of an isoscalar target it is strongly suppressed in the energy and momentum transfer regions under discussion. According to the symmetry properties of the background coherent reaction $\gamma A \rightarrow \pi^0 \pi^0 A$ on isoscalar nuclei [24], the two π^0 mesons prefer to propagate together in the CMS. The Monte-Carlo simulation shows that the additional suppression of the background to the level lower than the Coulomb photoproduction can be easily achieved using some angle cutoffs. To extract the signal of Coulomb photoproduction is possible in the experiment where a silicon detector is used as a sensitive target to develop a trigger on the nucleus recoil momentum.

Summarizing, we have found that for energies of the incident photon $\varepsilon \leq 4$ GeV and for momentum transfers $|\mathbf{q}_2| \leq 200$ MeV, $\pi^0 \pi^0$ pairs with $2m_\pi \leq m_{\pi\pi} \leq 700$ MeV in the reaction $\gamma A \rightarrow \pi^0 \pi^0 A$ are produced with a cross section of typically $\sigma \approx 40$ pb and $\sigma \approx 120$ pb for carbon and silicon nuclei, respectively. Our results demonstrate that this reaction can be experimentally investigated with presently available photon beams as a new source of the low-energy data on the process $\gamma\gamma \rightarrow \pi^0 \pi^0$.

Acknowledgments

The authors gratefully acknowledge fruitful discussions with G Anton, V V Burov, S S Kamalov, V K Lukyanov, G I Lykasov, B Mayer, E Oset and A V Tarasov.

References

- [1] Antipov Yu M *et al* 1983 *Phys. Lett.* **B121** 445
— 1984 *Z. Phys.* **C24** 39
- [2] Crystal Ball Collaboration (Marsiske H *et al*) 1990 *Phys. Rev.* **D41** 3324
- [3] Pennington M R 1992 *The DAΦNE Physics Handbook* vol II eds L Maiani, C Pancheri and N Paver (Frascati: INFN) p 379
- [4] Gasser J and Leutwyler H 1984 *Ann. Phys.* **158** 142
— 1985 *Nucl. Phys.* **B250** 465
- [5] Bijmens J and Cornet F 1988 *Nucl. Phys.* **B296** 557
Donoghue J F, Holstein B R and Lin Y C 1988 *Phys. Rev.* **D37** 2423
- [6] Bijmens J, Dawson S and Valencia G 1991 *Phys. Rev.* **D44** 3555
- [7] Donoghue J F and Holstein B R 1993 *Phys. Rev.* **D48** 137
Morgan D and Pennington M R 1991 *Phys. Lett.* **B272** 134
- [8] Bellucci S, Gasser J and Sainio M E 1994 *Nucl. Phys.* **B423** 80; *ibid* **B431** 413 (Erratum)
- [9] Knecht M, Moussallam B and Stern J 1994 *Nucl. Phys.* **B429** 125
- [10] Bellucci S and Bruno C 1994 Report BUTP-94/26, hep-ph/9502243
- [11] Bel'kov A A, Lanyov A V and Scherer S 1996 *J. Phys.* **G22** 1383
- [12] Bel'kov A A and Pervushin V N 1984 *Sov. J. Nucl. Phys.* **40** 616
- [13] Akhiezer A I and Berestetskii V B 1964 *Quantum Electrodynamics* (Moscow: Nauka); English translation 1965 (New York: Interscience) p 609
- [14] Fäldt G, Julius D, Pilkuhn H and Müllensiefen A 1972 *Nucl. Phys.* **B41** 125
- [15] Bijmens J, Bruno C and de Rafael E 1993 *Nucl. Phys.* **B390** 501
- [16] Bel'kov A A, Lanyov A V, Schaale A and Scherer S 1995 *Acta Physica Slovaca* **45** 121, hep-ph/9408368
- [17] Fearing H W and Scherer S 1996 *Phys. Rev.* **D53** 315
- [18] Volkov M K 1968 *Ann. Phys.* **49** 202
— 1974 *Fortschr. Phys.* **22** 499
- [19] Lüke L and Söding P 1971 *Springer tracts in modern physics* (Springer, Berlin) p 39
- [20] Gomez Tejedor J A and Oset E 1994 *Nucl. Phys.* **A571** 667
- [21] Gomez Tejedor J A and Oset E 1996 *Nucl. Phys.* **A600** 413
- [22] Braghieri A *et al* 1995 *Phys. Lett.* **B363** 46
- [23] Lukyanov V K and Pol Yu S 1974 *Fiz. Elem. Chastits At. Yadra* **5** 955 [1974 *Sov. J. Part. Nucl.* **5**]
Burov V V, Lukyanov V K and Pol Yu S 1976 *JINR preprint* P4-9556, Dubna
- [24] Oset E and Kamalov S S 1996 *Preprint* FTUV/96-86, IFIC/96-95

Figures

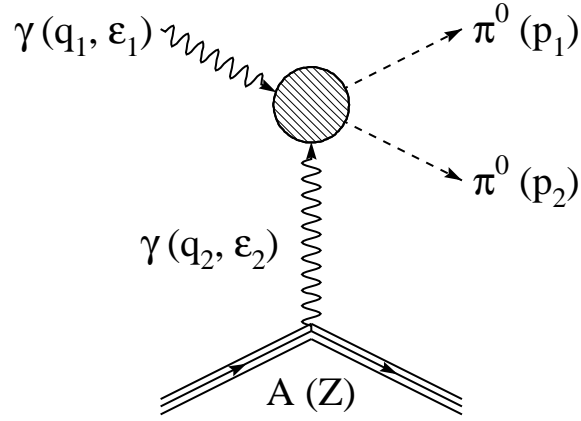


Figure 1. Photoproduction of pion pairs in the Coulomb field of a nucleus.

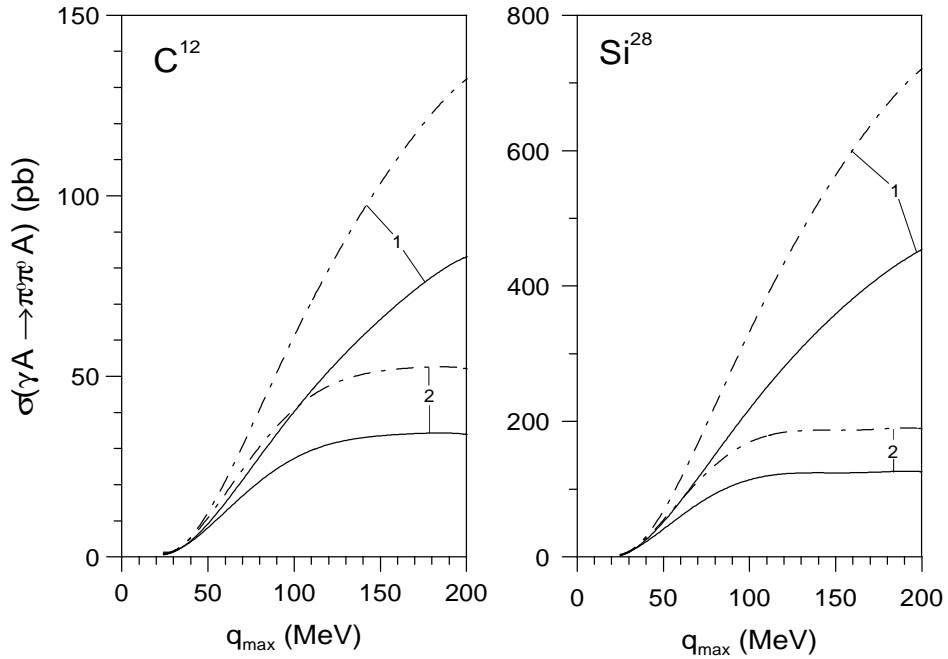


Figure 2. Dependence of the $\gamma A \rightarrow \pi^0 \pi^0 A$ cross section on the momentum transfer cutoff q_{\max} for the energy $\varepsilon = 4$ GeV of the incident photon. Compared are: L_i, d_i from the bosonization of the NJL model ([11], full curves) and from phenomenology ([8], dash-dotted curves), without and with a nuclear form factor (indicated by (1) and (2)).

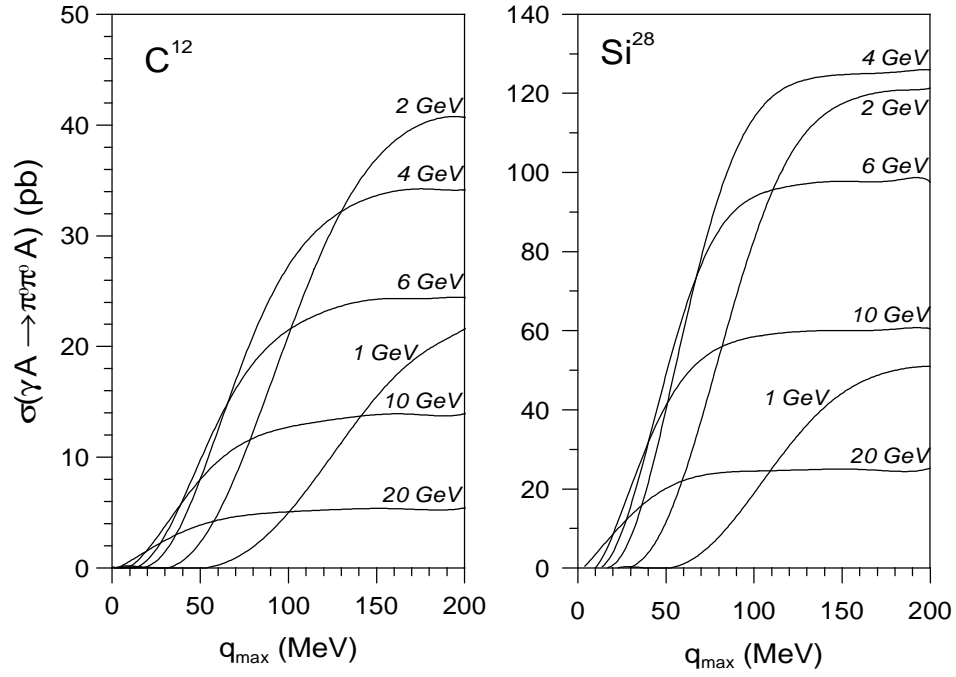


Figure 3. Dependence of the $\gamma A \rightarrow \pi^0 \pi^0 A$ cross section on the momentum transfer cutoff q_{\max} for different photon energies, with parameters L_i and d_i from the NJL model [11].

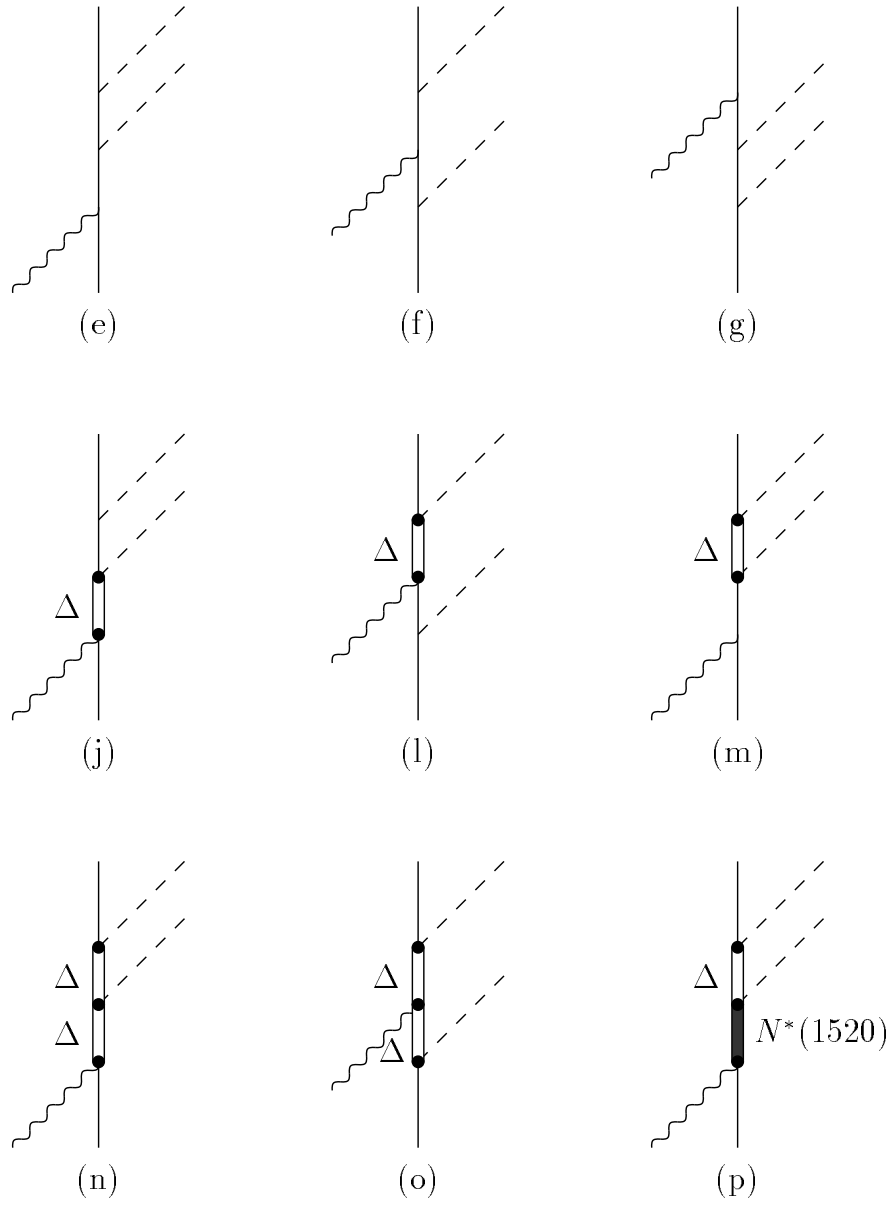


Figure 4. Dominating Feynman diagrams for the $\gamma p \rightarrow \pi^0 \pi^0 p$ and $\gamma n \rightarrow \pi^0 \pi^0 n$.

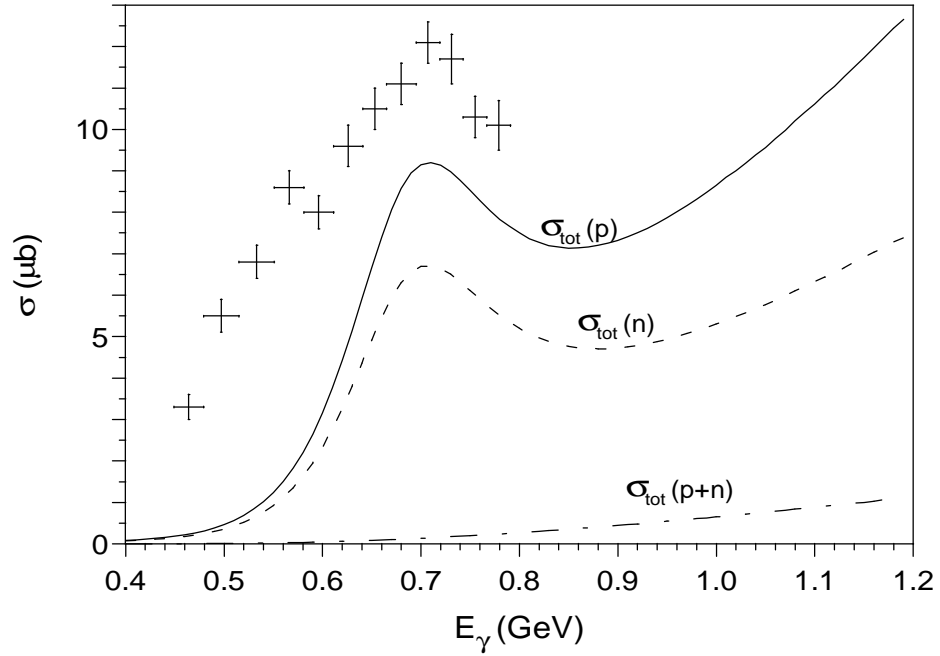


Figure 5. Total cross sections of the reactions $\gamma p \rightarrow \pi^0 \pi^0 p$ (full curve) and $\gamma n \rightarrow \pi^0 \pi^0 n$ (dashed curve) calculated in the framework of baryon resonance model [21] with diagrams of figure 4. Dash-dotted curve corresponds to the total cross section for the sum of the amplitudes on the proton and neutron. The experimental points for the reaction $\gamma p \rightarrow \pi^0 \pi^0 p$ were measured at DAΦNE [22].

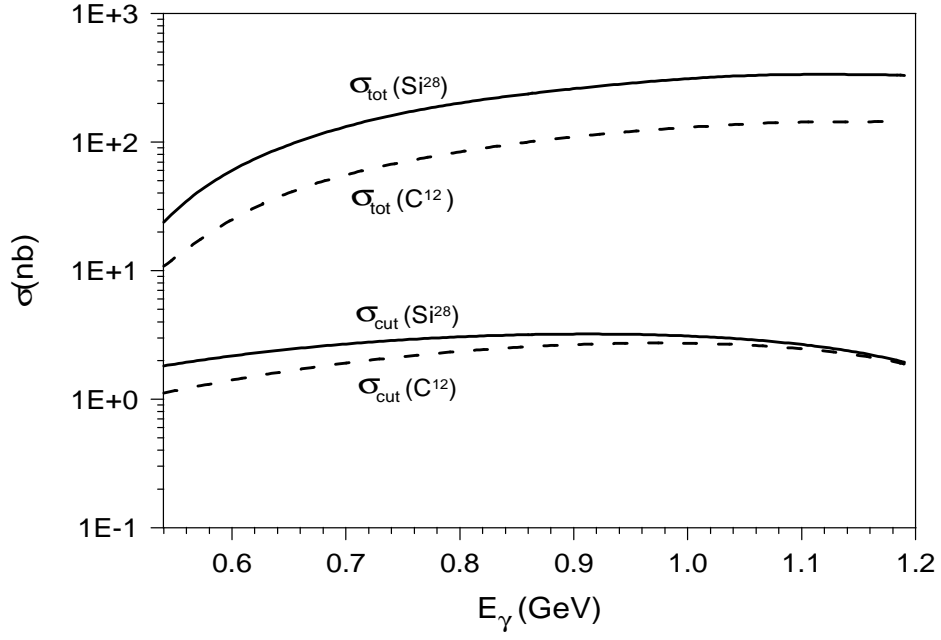


Figure 6. Total cross sections of the double pion photoproduction reaction (σ_{tot}) and cross sections calculated with the cutoffs $\sqrt{-t_N} \leq 150$ MeV and $m_{\pi\pi} \leq 700$ MeV (σ_{cut}) for coherent processes on the carbon (dashed curve) and silicon nuclei (full curve).